scientific reports

Check for updates

OPEN

Metabolomic insights into residual Carrot biomass from a bioprospecting approach across Colombian microclimates

Jaison Martínez-Saldarriaga[1]✉, Adriana Gallego[3], Felipe López-Hernández[1], Edith Marleny Cadena-Chamorro[4], Diana Paola Yepes-Betancur[5] & Juan Camilo Henao-Rojas[1,2]✉

Approximately 30% of global carrot *(Daucus carota)* production is discarded, illustrating a significant example of food loss and waste within the supply chain. Rather than being sent to landfills, where discarded carrots contribute to environmental issues such as greenhouse gas emissions and incur disposal costs, they could serve as valuable sources of high-value commercial metabolites. The present study employs metabolomic analysis to explore bioprospecting of discarded carrot biomass sourced from three Colombian locations, contributing to reduced food waste and supporting a circular economy approach. This study investigates the metabolomic profiles of different carrot types—cracked (R), deformed (D), pathologically damaged (P), and healthy controls (C)—from distinct locations: Marinilla, El Santuario, and Rionegro located in the department of Antioquia- Colombia. These locations, with their unique climatic conditions, influenced the metabolomic composition of the residual carrots. Notably, Nuciferine and Cryptotanshinone were more abundant in the Rionegro and El Santuario carrots. At the same time, 4′-Methoxyflavonol, N-Hexadecanoylpyrrolidine, Microcystin LW, and Feruloyltyramine were found in higher concentrations in carrots from Marinilla. Moreover, Marinilla exhibited more metabolic diversity than Rionegro and El Santuario. The study also discusses the bioprospecting potential of these metabolites in residual carrots, highlighting their possible applications as well as waste valorization.

Keywords Carrot, Bioprospecting, Re-valorization, Residual biomass, Metabolomic, Metabolite, Microclimate.

Carrots are an excellent source of carotenoids, vitamins, dietary fiber, minerals, and antioxidants, making them a highly nutritious and versatile food[1,2]. Globally, they are among the ten most widely produced and consumed vegetables[3]. The global carrot market, in terms of exports, is currently valued at $1.6 billion[4], and carrots are a significant source of employment for farmers; in fact, vegetable production provides approximately 300,000 direct and indirect jobs in Colombia[5].

With the population increase, global food demand is putting strong pressure on current agricultural systems. Parallelly, food loss and waste also increase in the food supply chain. Researchers estimate that the global percentages of food loss in production, postharvest, and consumption stages are 24, 24, and 35%, respectively[6]. Carrot production has increased in recent decades, reaching 41.7 million tons worldwide in 2021[4] . However,

[1]Centro de Investigación La Selva, Corporación Colombiana de Investigación Agropecuaria–Agrosavia, Kilómetro 7, Vereda Llanogrande, Vía a Las Palmas, Rionegro 054048, Colombia. [2]Grupo de Investigación en Sustancias Bioactivas GISB, Facultad de Ciencias Farmacéuticas y Alimentarias, Universidad de Antioquia, Cl. 70 No. 52-21, Medellín 0500100, Colombia. [3]BIOMASNEST SAS, Diagonal 74 C 32 B 94, Medellín, Colombia. [4]Facultad de Ciencias Agrarias, Departamento de Ingeniería Agrícola y Alimentos, Universidad Nacional de Colombia, Sede Medellín, Calle 59A N°63– 20, Medellín, Colombia. [5]Centro de la Innovación, Servicio Nacional de Aprendizaje (SENA), la Agroindustria y la Aviación, Cra48 N°49-62, Rionegro, Colombia. ✉email: jmartinezs@agrosavia.co; jhenao@agrosavia.co

approximately 30% of total carrot production is discarded during the postharvest stage, as it does not meet the quality standards required for commercialization, including reduced size, irregular length, inconsistencies in shape, color, and the presence of mechanical damage[7]. Consequently, there are approximately 12.51 million tons of discarded biomass potentially usable by carrot value chain. In rural areas where carrots are commonly grown, the residual biomass is often used as animal feed or compost material. On the other hand, it is incinerated or disposed of in open fields, negatively impacting the environment by contributing to air pollution and groundwater contamination[8,9]. Additionally, this leads to economic losses for producers and additional costs associated with disposing of discarded material, potentially discouraging agricultural efforts. Reducing the amount of organic waste generated, in terms of losses and production surpluses, can improve food security without increasing the environmental burden of agricultural practices[3].

Colombia's agricultural vocation makes it an interesting model for exploring waste valorization strategies, especially in the case of carrots, where losses reach around 30% in the country—similar to figures reported globally. In Colombia, carrots are classified into three categories for commercialization purposes. The first category, labeled "extra", includes carrots free from morphological defects, with regular shape, and without bruises or fissures. The second category, labeled "first," includes carrots with a good appearance but allows minor defects, such as handling or washing-related injuries. Finally, the "second" category includes carrots with defects such as healed wounds and burn marks[10,11]. Carrots are discarded and considered residual biomass or surplus production when quality variations arise, such as cracked, deformed, or pathologically damaged. These surpluses have been considered renewable and abundant sources of chemical compounds of interest and have even been used as raw materials in biorefinery processes focused on producing fermentable sugars, carotenoids, and biofuels[7,12,13].

The utilization of food waste as a source for recovery of value-added compounds through sustainable technologies and bioprospecting is key to improving food security and having a sustainable environment, as food losses contribute to the release of greenhouse gases, poor air quality, land, and water pollution[14]. Food waste can serve as a platform for chemicals, nutraceuticals, sugars, biofuels, biogas, and biochar via thermochemical conversion, anaerobic digestion, and fermentation processes. Now, food waste may start at the source of origin where the harvest is done, and farmers select which products are suitable for commercial purposes; for this reason, the use of agricultural wastes and rejects allows not only nutritional recovery but also economic gain for the producer[3,7]. At the same time, plant metabolism is influenced by local changes in temperature, water availability, and atmospheric CO_2 concentration[15]. Then, understanding how the local environment influences the biochemical profile of food waste is crucial to determining its potential in bioprospecting and waste valorization.

The chemical composition of an agro-food matrix, such as carrots, may vary due to factors associated with the growing location and their microclimates. The number, proportions, composition, and quality of chemical compounds in plants are influenced by various environmental factors, including geographic location, solar radiation, precipitation, and average temperature, which in intertropical regions like Colombia are primarily determined by altitude. These factors can directly or indirectly affect the concentration of secondary metabolites, and the biological activity associated with these compounds[16–18]. Several studies have explored food matrices such as mint, mango, or dragon fruit, determining a direct influence of altitude and other climate characteristics on levels of phenolic compounds, flavonoids, alkaloids, amino acids, among others, and their inherent bioactivities[16–20]. However, few studies have focused on evaluating the chemical variability of organic waste, losses, and production surpluses concerning their locality, especially in residual carrots; therefore, it is necessary to consider the high crop heterogeneity and their chemical variability influenced by locality, along with the issues related to underuse of carrot crop surpluses, such as the decrease in production yields in harvests and the inherent losses for producers[7,12], as a possible opportunity to find cultivation areas with differential qualities[18,19] and achieve the whole production use.

Based on the above, it is essential to conduct bioprospecting studies to identify molecules of interest in residual carrot biomass, facilitating the determination of new uses and discovering specific markets and production niches. For instance, production surpluses with higher carotenoid content could be used specifically in natural colorant production, bioactive ingredients in pharmaceuticals, and cosmetic compounds[12,21]. Alternatively, production surpluses from a particular locality with higher phenolic and/or antioxidant content could be directed towards generating functional ingredients for various applications[8,22] or for fermentation or biorefinery processes if a higher content of fermentable sugars or polysaccharides is identified[7,22]; thus adding value to the production chain and enabling the replication of such applications or transformations in different localities under similar climate conditions.

Bioprospecting studies can be conducted through metabolomic techniques, which enable high-resolution phenotypic identification[23]. Metabolomics is the comprehensive study of low-molecular-weight metabolites in a biological system[24]. Metabolomics, therefore, provides a broad profile of the metabolic richness of a food matrix[25]. The recent advances in analytical techniques, such as liquid chromatography coupled with mass spectrometry (LC-MS), allow for the identification of hundreds of metabolites and the evaluation of differences and similarities between samples[26]. Indeed, lipidomic techniques, well known as a subfield of metabolomics[25,27], may be seen as a key tool to decipher the metabolite composition of carrots, having into account there are an essential amount of lipid-based compounds associated with color and antioxidant activity, such as carotenoids[21,28]; however, there are few lipidomic studies on carrots that focus on evaluating agroecological effects on the metabolome[29,30], and none so far related to carrot residues, surpluses, or residual biomass. This study aims to determine the effect of microclimate in the metabolic profiles of four types of carrot biomass—cracked (R), deformed (D), and pathologically damaged (P) and control without damages (C)—collected from three distinct localities in the eastern municipalities of the Department of Antioquia, Colombia: Rionegro, Marinilla, and El Santuario. Each locality presents unique climatic conditions; thus, understanding how these climatic gradients influence

the metabolic profiles of residual biomass can provide valuable insights in bioprospecting. Furthermore, this knowledge may help in reducing losses and optimize processes in the food supply chain and facilitates the development of targeted strategies to enhance the re-valorization of agro-industrial waste. Such advancements contribute to shifting from a linear production model to a circular economy approach, promoting sustainability and efficiency[9]. Finally, the findings of this study could support the replication of bioprospecting initiatives across other regions under similar climatic conditions, enabling the generation of bioactive compounds for diverse applications in pharmaceuticals, nutraceuticals, and agro-industrial processes.

Materials and methods

Plant material sampling

Carrot (*Daucus carota L.)* samples of the Bangor variety were harvested four months after planting from three different localities in Antioquia (Colombia): El Santuario (6°9'12"N, 75°16'38,6"E), Marinilla (6°11'8,5"N, 75°15'26"E), and Rionegro (6°7'53,876"N, 75°24'52,166"E), collected in November 2023 (Fig. 1A.). One general sampling of production surpluses was performed at each locality, considering four carrot types to know: control (C), carrots with conical shape without secondary roots or branches, free from spots, fissures, or wounds (Fig. 1B.); cracked (R), carrots with superficial damage in the form of fissures (Fig. 1C.); deformed (D), showing evident malformations or bifurcated appearance (Fig. 1D.); and pathologically damaged (P), carrots with superficial deterioration associated with color changes or the appearance of spots caused by pathogen attacks (Fig. 1E.).

Climatic data collection

The climatic characteristics of the three localities are presented in Table 1. For each georeferenced sampling point, we obtained high-resolution climatic variables from the CHELSA v2.1 platform (https://chelsa-climate.org/), which provides spatially interpolated monthly climate data at ~ 1 km² resolution. Specifically, we extracted data for the period 2009–2018, focusing on the months that matched the experimental sampling. Historical climatic datasets offer a robust baseline for ecological comparisons, particularly relevant here since the agricultural materials have long adapted to local climatic conditions[31]. An analysis of mean differences for each climatic variable across localities was conducted using ANOVA, followed by Tukey's post-hoc test to identify significant differences between microclimates. In addition, an altitudinal gradient analysis was performed using the *rast* and *ggplot2* functions (R environment, https://cran.r-project.org/bin/windows/base/) aligned with the climatic data set described above.

Sample Preparation

Five kilograms of carrots were harvested and processed for each residual biomass typology at each of the three localities. The carrots were thoroughly washed, disinfected by immersion in a sodium hypochlorite solution (200 ppm for 5 min), and then rinsed to remove the excess of disinfectant. Carrots were peeled, and crowns and tips were removed. The carrots were then chopped and homogenized using an industrial blender (Oster; Milwaukee, WI, USA); until the particle size was less than 1 cm³. From this material, 300 g were lyophilized at -50 °C for 40 h (Biobase; Jinan, China), yielding approximately 30 g. This process was performed in quadruplicate. The lyophilized material was stored under vacuum in multilayer laminated bags (aluminum/polyethylene/low-density polyethylene) at -20 °C until extraction.

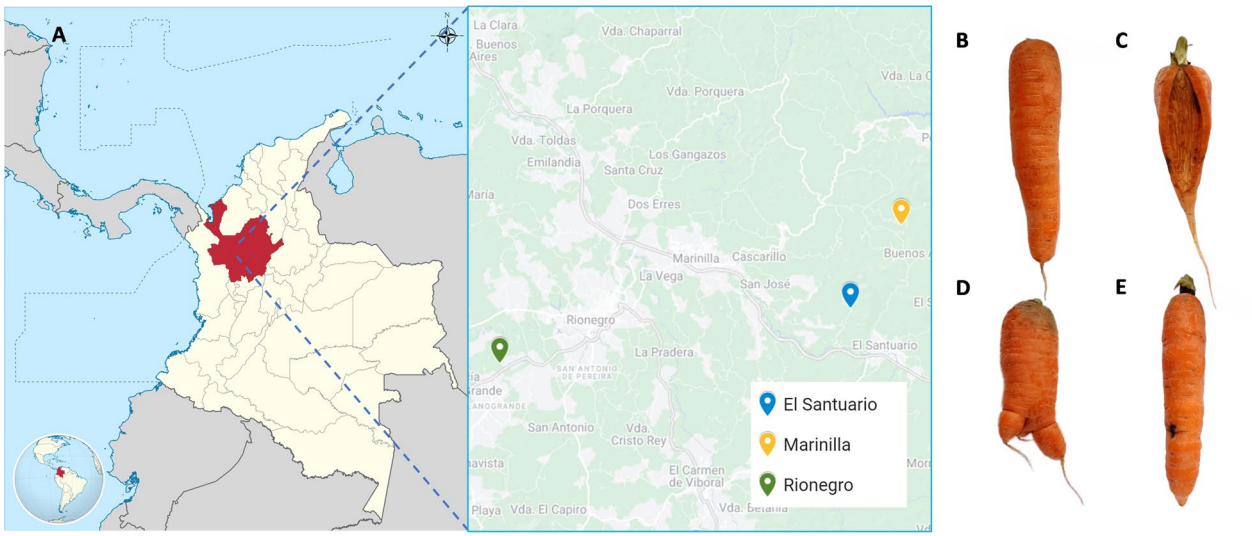

Fig. 1. Georeferenced map of the harvesting locations (A) and carrot residual biomass typologies analyzed: Control (B), Cracked (C), Deformed (D), Pathologically damaged (E). Map acquired under the Creative Commons Attribution-Share Alike 3.0 Unported license, source from: https://commons.wikimedia.org/wiki/File:Colombia_-_Antioquia.svg#.

Climatic Characteristics	Localities		
	Marinilla	El Santuario	Rionegro
Altitude (m.a.s.l.)	2284.0 ± 0.0	2160.0 ± 0.0	2119.0 ± 0.0
Precipitation (mm)	2929.085 ± 0.0	2752.389 ± 10.925	2536.944 ± 12.218
Near-surface relative humidity (%)	66.759 ± 0.0	66.535 ± 0.008	67.683 ± 0.068
Daily minimum near-surface air temperature (°C)	28.408 ± 0.0	28.487 ± 0.005	28.514 ± 0.005
Daily maximum near-surface air temperature (°C)	29.296 ± 0.0	29.387 ± 0.007	29.452 ± 0.006
Near-surface air temperature (°C)	28.915 ± 0.0	29.000 ± 0.007	29.048 ± 0.006
Vapor pressure deficit (kPa)	0.610 ± 0.0	0.647 ± 0.002	0.643 ± 0.001
Surface downwelling shortwave radiation (MJ/m^2)	1.815 ± 0.0	1.862 ± 0.001	1.898 ± 0.003
Near-surface wind speed (m/s)	2.008 ± 0.0	1.232 ± 0.071	1.566 ± 0.052
Potential evapotranspiration (mm/day)	1151.500 ± 0.0	1167.840 ± 13.053	1224.506 ± 4.686
Cloud area fraction (%)	79.255 ± 0.0	77.679 ± 0.0	75.310 ± 0.0
Climate moisture index	1777.578 ± 0.0	1584.5209 ± 24.026	1312.535 ± 7.860

Table 1. Climatic characteristics of the evaluated harvested localities.

A total of 10 mg of each lyophilized sample was mixed with 150 µL of cold acetone and homogenized by vortexing for 30 s (DLab Scientific; Beijing, China); acetone was selected as the extraction solvent aligned with a lipid-oriented untargeted metabolomic profile (lipidomic), due to its ability to solubilize semi-polar and moderately non-polar metabolites, including carotenoids, fatty-acid derivatives, alkaloids, phenolic derivatives, amides, and other lipid-related secondary metabolites known to occur in carrot tissues. The sample was centrifuged at 27,000 xg (16000 rpm) for 10 min at 4 °C (Thermo Fisher Scientific; Waltham, MA, USA). The supernatant was recovered, and another 150 µL of cold acetone was added to the precipitate, repeating twice the process. The three supernatants were combined and transferred to an Eppendorf tube. A 300 µL aliquot of supernatant was mixed with 300 µL of MTBE and vortexed for 5 s; then, 100 µL of water was added and vortexed for 5 s. The mixture was centrifuged at 27,000 xg (16000 rpm) for 10 min at 4 °C. The supernatant was recovered, and another 150 µL of MTBE was added to the precipitate, repeating twice the extraction process. The resulting extract, containing an acetone: MTBE solvent mix, was filtered using a 0.2 µm acrodisc filter.

LC/MS and RP-LCMS/MS-QTOF conditions

Metabolomic analysis was performed using an Agilent Technologies 1260 liquid chromatography system coupled with a Q-TOF 6545 quadrupole time-of-flight mass analyzer with electrospray ionization (Agilent Technologies, Palo Alto, CA, USA). One µL of each metabolite extract was injected into a C18 column (InfinityLab Poroshell 120 EC-C18 (100 × 3.0 mm, 2.7 µm)) at 50 °C, with an elution gradient of ammonium acetate solution (10 mM) dissolved in an H2O mix (90:10) (phase A) and ammonium acetate solution (10 mM) dissolved in an ACN: MeOH mix (20:30:50) (phase B), with a constant flow rate of 0.6 mL/min. Mass spectrometry detection was performed in positive ESI mode in a full scan from 100 to 1700 m/z. During analysis, a mass reference mixture was calibrated: m/z 121.0509 ($C_5H_4N_4$) and m/z 922.0098 ($C_{18}H_{18}O_6N_3P_3F_{24}$). The chromatographic elution gradient began with 70% of phase B for 1 min, increased to 86% of phase B over 3.5 min, remaining in these conditions for 6.5 min; then increased to 100% of phase B in 1 min and held for 6 min. Afterward, it returned to the initial conditions in 0.1 min and was equilibrated for 3 min.

ESI-MS/MS analyses were performed in positive ionization mode with a full scan from 100 to 1700 Da. The ESI-QTOF-MS/MS was operated under the following conditions: Dual AJS ESI source, Vcap 3500 V, drying gas 10 L/min, gas temperature 200 °C, nebulizer 50 psi, sheath gas temperature 300 °C, and sheath gas flow rate 12 L/min. For MS-TOF, the conditions were: fragmentation 175 V, skimmer 65 V, and OCT RF Vpp 750 V. For MS/MS conditions, collision energy was set at 40 eV, scan range 100–1700 m/z, acquisition speed of 1 spectrum/s, and acquisition time of 1000 ms/spectrum. The runtime was 20 min. For quality control, a set of samples was measured at the beginning of the run. A QC group was prepared by mixing 150 µL of each sample, injecting two QCs at the beginning of the sequence and, subsequently, every four samples to ensure no analytical variability from the instrument. The samples were randomized using Excel's random function and injected in that order.

A re-fragmentation process was performed on a series of previously selected masses based on their abundance levels or degree of significance. For this purpose, the samples were analyzed using identical liquid chromatography and mass analyzer system configurations. One µL of extracts was injected into a C18 column (100 × 3.0 mm, 2.7 µm) at 60 °C, with a gradient elution composed of 10 mM ammonium formate in 60:40 CAN plus 0.1% formic acid (Phase A) and 10 mM ammonium formate in IPA 90:10 plus 0.1% formic acid (Phase B), at a constant flow rate of 0.6 mL/min. Mass spectrometry detection was performed in positive ESI mode. For mass correction, two reference masses were used during the entire analysis: m/z 121.0509 ($C_5H_4N_4$) and m/z 922.0098 ($C_{18}H_{18}O_6N_3P_3F_{24}$). The directed MS/MS analysis was set to a collision energy of 20 V, and the chromatographic elution gradient started with 15% of Phase B, increasing to 30% over 2 min, then reaching 48% over another 2.5 min, subsequently increasing to 82% over 11 min and then to 99% over 23.5 min. Finally, the gradient decreased to 15% in an initial stage of 12.1 min and a final stage of 18 min. Method adapted from previous proposed methodologies[32].

Metabolomic data processing and analysis

The compounds present were analyzed and manually inspected using Agilent MassHunter Profinder software, version 10.0, employing the Recursive Molecular Extraction algorithm with an extraction time of 17 min, 5000 counts, using positive ion species (+H, +Na, -H_2O, NH_4, K) and without applying mass or signal filters. This algorithm deconvolutes the chromatogram and integrates the molecular features in the samples and solvent blank based on mass and retention time. The results obtained were subjected to a reproducibility-based filtering process; during this procedure, the area's coefficient of variation (CV) in the quality control (QC) samples was calculated, and molecular properties with a CV higher than 20% were excluded.

Initial MS data was converted to mzXML format using ProteoWizard (https://proteowizard.sourceforge.io/) and then to abf files using ABF converter (https://www.reifycs.com/AbfConverter/). Data analysis was conducted using MS-DIAL software (http://prime.psc.riken.jp/compms/msdial/main.html) with the following parameters: mass range (0-2000 Da), MS1 alignment tolerance (0.01 Da), MS2 alignment tolerance (0.025 Da), retention time (0–100 min), minimum peak height (1000), sigma (0.5), and MS accurate mass tolerance (0.015 Da). Method adapted from previous proposed methodologies[32].

The confirmation of statistically significant molecular features was achieved during the re-fragmentation process by determining the exact mass, the molecular formula, and the mass spectra analysis. The annotation involved a combination of platforms, including MS-DIAL 5.0 using libraries from MoNA - MassBank of North America: MoNA-export-LC-MS/MS_Positive_Mode, MoNA-export-GNPS, and MoNA-export-Vaniya-Fiehn_Natural_Products_Library, as well as SIRIUS 5.8.6 software, and in silico tools like CFM ID (cfmid3.wishartlab.com/). Additionally, the refragmented masses were reviewed one by one using their m/z values and intensities or retention times against complementary databases such as MassBank (https://massbank.eu/MassBank/), LipidMaps (https://lipidmaps.org/), Plant Metabolome Repository (https://metabolites.in/plants/), and CEU Mass Mediator (https://ceumass.eps.uspceu.es/index.xhtml), employing spectral, similarity, peak, and other searches with a threshold of at least 0.80 or tolerances no greater than 10 ppm in peak masses. Each metabolite was reported with an ID confidence level according to the Metabolomics Standards Initiative (MSI) guidelines, where Level 0 indicates an unequivocal 3D structure, Level 1 a reliable 2D structure compared with a reference standard, Level 2 a probable structure corroborated by literature or database evidence, Level 3 a possible structure or class identified by molecular formula, and Level 4 an unidentified feature that indicates presence without specific identification.

Metabolite enrichment analysis

The retrieved annotated metabolite list was subjected into MetaboAnalyst 6.0 (https://www.metaboanalyst.ca/) for an Over Representation Analysis (ORA) and metabolic pathway enrichment analysis. The overall annotation of metabolite features was performed by "Annotated Features" module using "Pathway Enrichment" and "Network Analysis" sub-modules, by the RaMP-DB (metabolite and lipid pathways, integrating KEGG via HMDB, Reactome and WikiPathways) pathway-based metabolite library. Target analysis was done with *Arabidopsis thaliana* from the Kyoto Encyclopedia of Genes and Genomes (KEGG) database as the target organism[33–35].

Metabolomic statistical analysis

Abundance peaks from the final identification and metabolites were exported from MS-DIAL and subjected to multidimensional statistical analysis using MetaboAnalyst 6.0 (https://www.metaboanalyst.ca/), by the "Statistical Analysis" module and the "one factor" sub-module. The data were preprocessed before performing multidimensional statistical analysis, no missing values were detected from the original dataset, and there was no data filtering. The different normalization procedures were performed, and all the data scaling, transformation, and normalization were tested in order to find the best model for representing the data and its variability. Therefore, the data were preprocessed through median normalization, log transformation (base 10), and Pareto scaling, followed by univariate and multivariate statistics. Univariate analysis included fold change (FC) analysis (FC threshold value = 2) to identify up and down-regulated metabolite features, and volcano plot (FC threshold value = 2 and *p-value* threshold = 0.05). Multivariate analysis included principal component analysis (PCA) and orthogonal partial least squares discriminant analysis (OPLS-DA) with a *p-value* threshold = 0.05; and a hierarchical clustering analysis (HCA), using normalized data and autoscale samples, additionally, having on count a euclidian distance and a ward clustering method. The VIP score obtained in the OPLS-DA model and fold-change facilitated the assessment of the influence of intensity and explanatory ability of each of the metabolites in classifying and discriminating clusters of samples on the basis of biologically significant metabolite features. The model parameters (R^2Y and Q^2) were calculated automatically as part of the OPLS-DA model evaluation, specifically, R^2Y represents the fraction of variation in the response variable explained by the model, while Q^2 indicates the model's predictive ability estimated by cross-validation.

Results

Exploratory analysis of microclimatic patterns

The climatic diversity across the three localities revealed distinct microclimatic clusters that may influence carrot metabolic profiles. The three localities—El Santuario, Marinilla, and Rionegro—in Antioquia, Colombia, exhibited unique climatic conditions, as detailed in Table 1. Marinilla, situated at the highest altitude, presented distinctive climatic characteristics, including the highest values for precipitation, wind speed, cloud area fraction, and climate moisture index. Rionegro and El Santuario, located at intermediate to lower altitudes, displayed similar climatic conditions driven by relative humidity, potential evapotranspiration, temperature-related variables, and solar radiation, suggesting moderate and less extreme variation for Rionegro and El Santuario.

Although each locality was localized at different altitudes, some climatic characteristics were shared between localities. Marinilla stood out with its higher wind speeds (2.008 m/s) and precipitation (2929.0 mm annually), emphasizing its wetter and windier climate compared to Rionegro and El Santuario. On the other hand, El Santuario clustered closer to Rionegro, indicating similar profiles with moderate to high temperatures, higher solar radiation, and a more significant vapor pressure deficit (0.647 and 0.643 kPa, respectively), indicative of less cloudy conditions and a warmer and drier microclimate compared to Marinilla. These patterns align with the altitudinal gradient shown in Fig. 2A, where Marinilla is located at a greater altitude (2284.0 m.a.s.l.) compared to El Santuario (2160.0 m.a.s.l.) and Rionegro (2119.0 m.a.s.l.), which highlights the relationship between elevation and climatic variation across El Santuario and Rionegro localities against Marinilla. [15,33,34]

Statistical analysis using ANOVA revealed significant differences in key climatic variables across the localities. Tukey's post-hoc test identified specific pairwise differences (Fig. 2B-G), thus reinforcing the distinctions associated with the altitude. Based on the above, we decided to group the localities into one cluster (C1) composed of Rionegro and El Santuario and a second cluster (C2) composed of Marinilla. The analyses further demonstrate that El Santuario and Rionegro can be grouped together based on their climatic similarities, whereas Marinilla exhibits distinct climatic profiles shaped by a unique combination of environmental factors. Climatic differences likely influence the metabolic profiles of residual carrot biomass samples. Factors such as altitude, temperature, precipitation, and other climatic characteristics, along with region-specific biotic factors (e.g., the influence of the growth locality), may explain variations in chemical composition and bioactive compounds[16,19]. Consequently, microclimatic diversity underscores the importance of considering local environmental conditions in agricultural and metabolic research.

The results demonstrate a marked differentiation in climatic conditions among the studied locations (Marinilla, Rionegro, and El Santuario). Marinilla, for instance, displays distinct climate characteristics, such as higher wind speed, precipitation, and cloud cover. Some of these climatic variables have been shown to significantly influence the biosynthesis of metabolites in organic waste, aligning with previous findings on the effects of climate on crop quality under abiotic stress[36]. In this context, clarifying which variables contribute most to climatic differentiation at both univariate and multivariate levels is essential to understanding their effect on the metabolomic profile of residual carrot biomass.

Metabolomic profile of residual carrots from different localities

The metabolomic profiles of different carrot types—cracked (R), deformed (D), pathologically damaged (P), and healthy as a control (C)—from various localities (Marinilla, El Santuario, and Rionegro) were evaluated (Supplementary Dataset S1). PCA analysis (Supplementary Fig. S1) did not reveal a clear separation among the carrot typologies. However, distinct clustering emerged when analyzing the climatic patterns of the three localities, which were analyzed independently through an exploratory multivariate analysis (PCA), revealing that Marinilla consistently separated from the other two localities, Rionegro and El Santuario (Supplementary Fig. S2).

A total of 90 metabolites were identified with level 2 and 3 identification confidence level (Supplementary Dataset S2); no metabolite was confirmed using verified reference standards, therefore the results should be interpreted cautiously. In addition, the chemical classes identified (carotenoids, fatty-acid derivatives, alkaloids, flavonoids, terpenoids, and other semi-polar compounds) are consistent with the solvent system extraction profile, indicating that it is appropriate for the targeted metabolomic analysis of residual carrot biomass. Data of abundance were analyzed through hierarchical cluster analysis (HCA) and orthogonal partial least squares discriminant analysis (OPLS-DA). Data of abundance from all experimental and quality control samples were subjected to OPLS-DA; the model was established by comparing Rionegro and El Santuario, designated as cluster 1 (C1), against Marinilla, designated as cluster 2 (C2). The model evaluation parameters were R^2Y with a value of 0.556 and Q^2 with 0.453, and a permutation test ($n = 100$) was conducted to assess the robustness and statistical significance of the OPLS-DA model (Suplementary Fig. S3).

The OPLS-DA score plot (Fig. 3A) shows a clear separation with a 95% confidence level between Marinilla carrot samples and those from Rionegro and El Santuario, indicating metabolic differences between the clusters. Marinilla samples are more tightly clustered, suggesting greater homogeneity regarding chemical richness or metabolomic characteristics. In contrast, samples from Rionegro and El Santuario show a greater dispersion, indicating a higher degree of metabolomic variability.

Additionally, Variable Importance in the Projection (VIP) values were generated to evaluate the overall metabolite impact on cluster differentiation. Metabolites with VIP values > 1 are the most influential for the model and were used to measure the strength and explanatory capacity of each metabolite's expression pattern in classifying and distinguishing between Rionegro and El Santuario against Marinilla. Figure 3B shows the top twenty VIP scores (VIP score > 1.0), with a p-value < 0.05. The metabolites with the highest VIP scores were Nuciferine, Feruloyltyramine, and Microcystin LW with VIP scores > 2.5, while Cryptotanshinone, N-Hexadecanoylpyrrolidine, and 4'-Methoxyflavonol with VIP score between 2.0 and 2.5, contributed most significantly to the differentiation between the clusters.

To more comprehensively, generally, and intuitively evaluate relationships between samples and differences in metabolite expression patterns in different clusters, data on relative metabolite abundances were analyzed through hierarchical clustering using a heatmap. This process allowed for more accurate identification of marker metabolites and, thus, a better understanding of the related metabolic processes. Grouped metabolites simultaneously showed similar expression patterns and could participate in closely related reaction steps in metabolic processes. Figure 3C illustrates the hierarchical clustering results of the top 28 VIPs. The color scale reveals a clear separation between C1 and C2, with some differential patterns. Specifically, Nuciferine and Cryptotanshinone were more abundant in C1 (Rionegro and Santuario), whereas 4'-Methoxyflavonol, N-Hexadecanoylpyrrolidine, Microcystin LW, and Feruloyltyramine showed higher abundance in carrots from

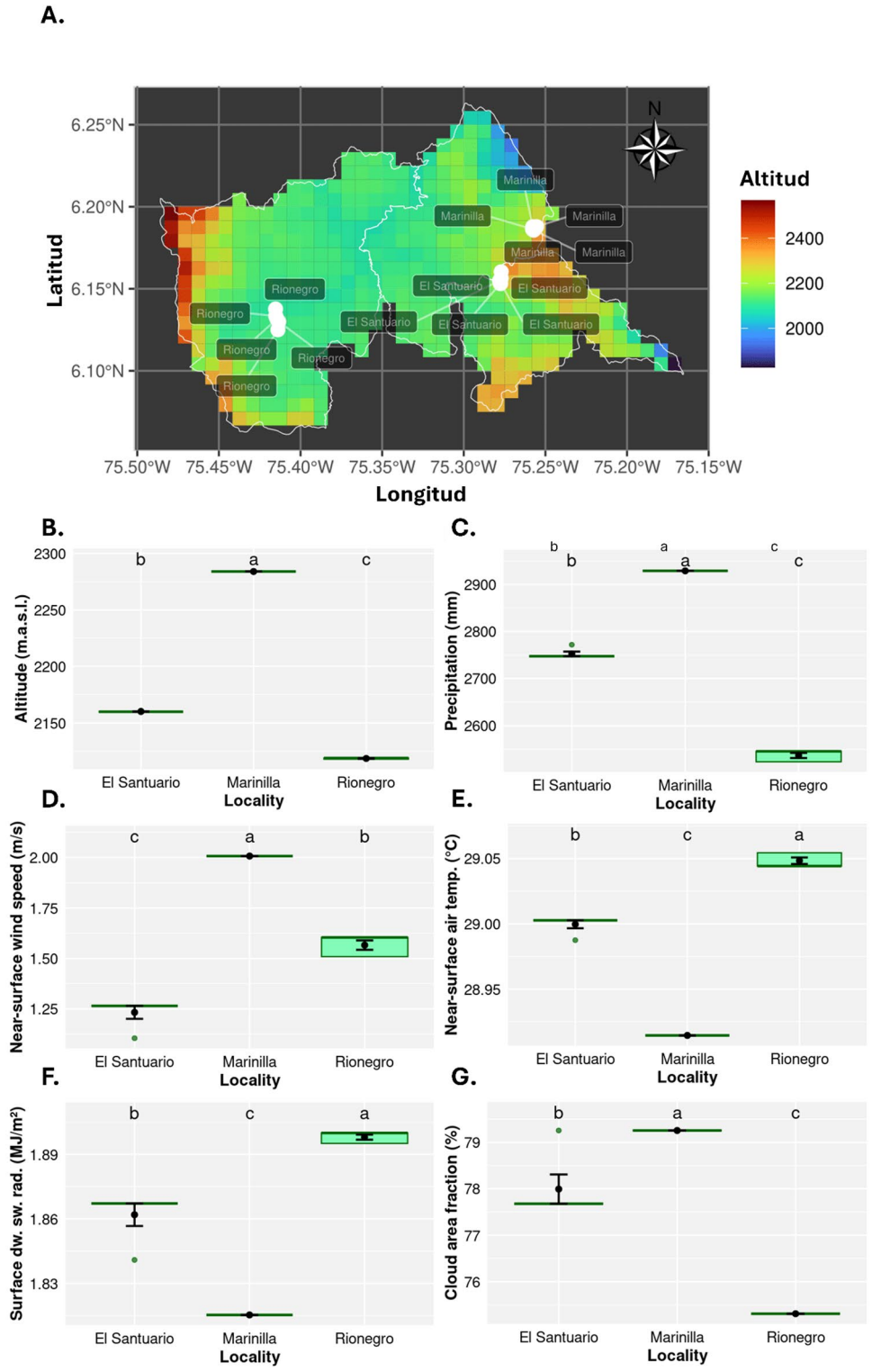

Fig. 2. Climate analysis associated with the three evaluated localities. Altitudinal gradient plot (A), and significant differences in key climatic variables, ANOVA analysis followed by Tukey's post-hoc test (B-G); altitude (B), precipitation (C), near-surface wind speed (D), near-surface air temperature (E), surface downwelling shortwave radiation (F), and cloud area fraction (G); different letters above each boxplot indicate statistically significant differences. Map generated from R software (version 4.5.1) by *ggplot2* and *raster* R packages (https://cran.r-project.org/bin/windows/base/).

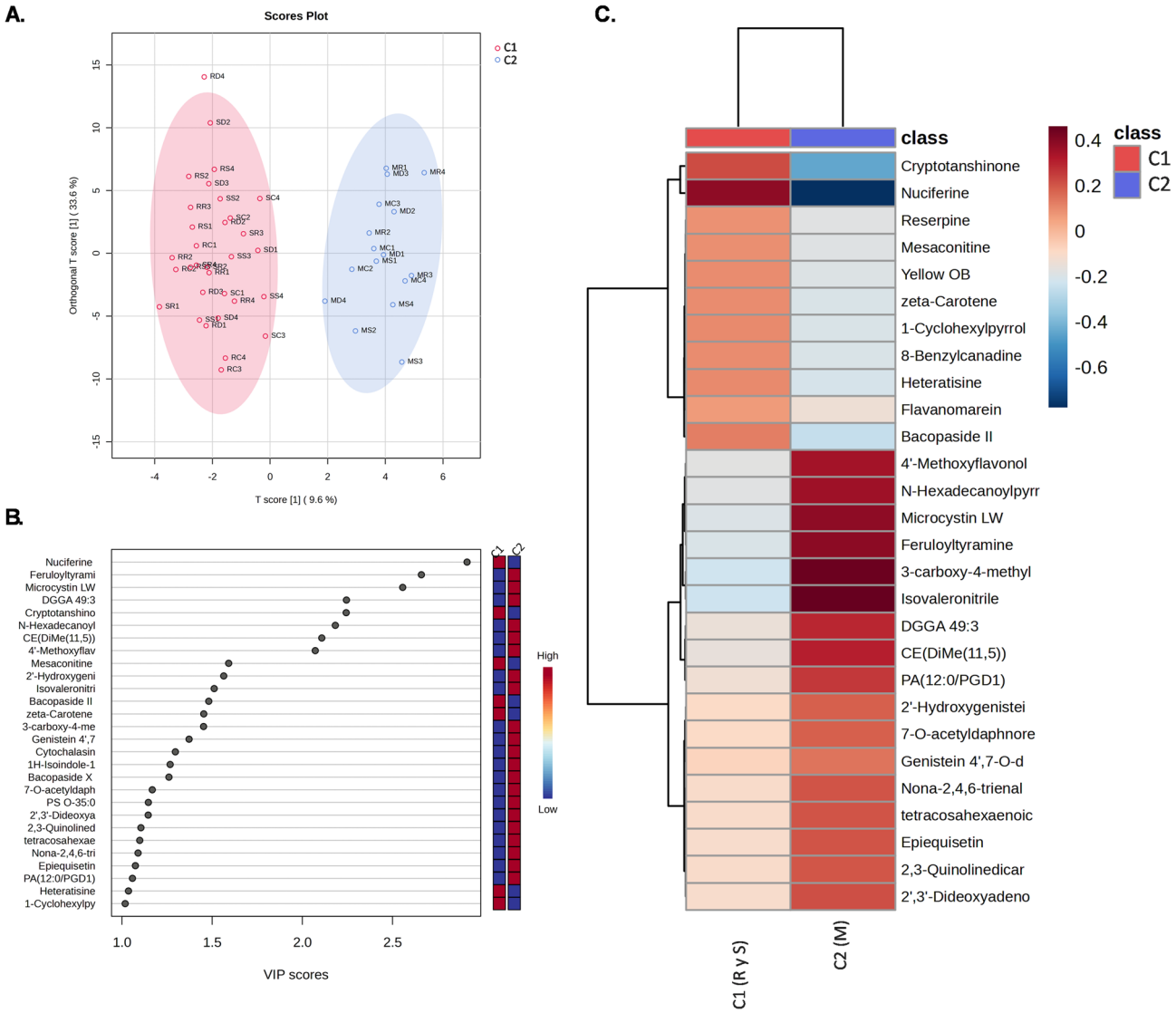

Fig. 3. OPLS-DA score plot (A), VIP score plot (B), and heatmap plot (C) between the Marinilla locality (C2) concerning Rionegro and El Santuario (C1).

C2 (Marinilla). Additionally, more metabolites were enriched in C2 of Marinilla than in C1 (Rionegro and Santuario)[15,16,19,30]. Furthermore, we evaluated the foldchange of the most important VIPs in the volcano plot. Here, colored dots represent metabolites with fold change (FC) > 1 or FC < -1 and a p-value threshold on FDR < 0.05, indicating differentially expressed metabolites; FC > 1 suggests an upregulation of the metabolite, and FC < -1 indicates downregulation of the metabolite. The univariate statistical analysis results are shown in Fig. 4.

The blue dots on the right side of the x-axis represent metabolites that are more abundant in C1 (Rionegro and El Santuario), such as Nuciferine with the highest foldchange value (> 2.5) and with a clear significant difference from superior abundance in C1 compared to C2. Cryptotanshinone with a fold change value between 1.0 and 1.5 stands out as the most significant metabolites in C1, suggesting a high accumulation of these compounds in those localities. This variability may be influenced by specific agroclimatic factors in Rionegro and Santuario that promote the accumulation of these metabolites, possibly related to environmental stress responses or unique cultivation conditions. On the left side of the x-axis, the more negative values indicate metabolites more abundant in C2 (Marinilla), such as Feruloyltyramine, Microcystin LW, N-Hexadecanoylpyrrolidine, and 4'-Methoxyflavonol, with foldchange values between −0.5 and −1, reporting the higher abundance values of in C2, and a significant difference concerning C1; especially, Feruloyltyramine and Microcystin LW which presented the highest abundance values in C2.

Additionally, a metabolic enrichment analysis was conducted to understand better the metabolic pathways associated with the identified metabolites, based on significance level (p-value < 0.05) and enrichment score. Figure 5 shows the most significant metabolic pathways, with the α-linolenic acid metabolism pathway at the top of the list, followed by the vitamin A and carotenoid metabolism pathway; these two primary pathways have

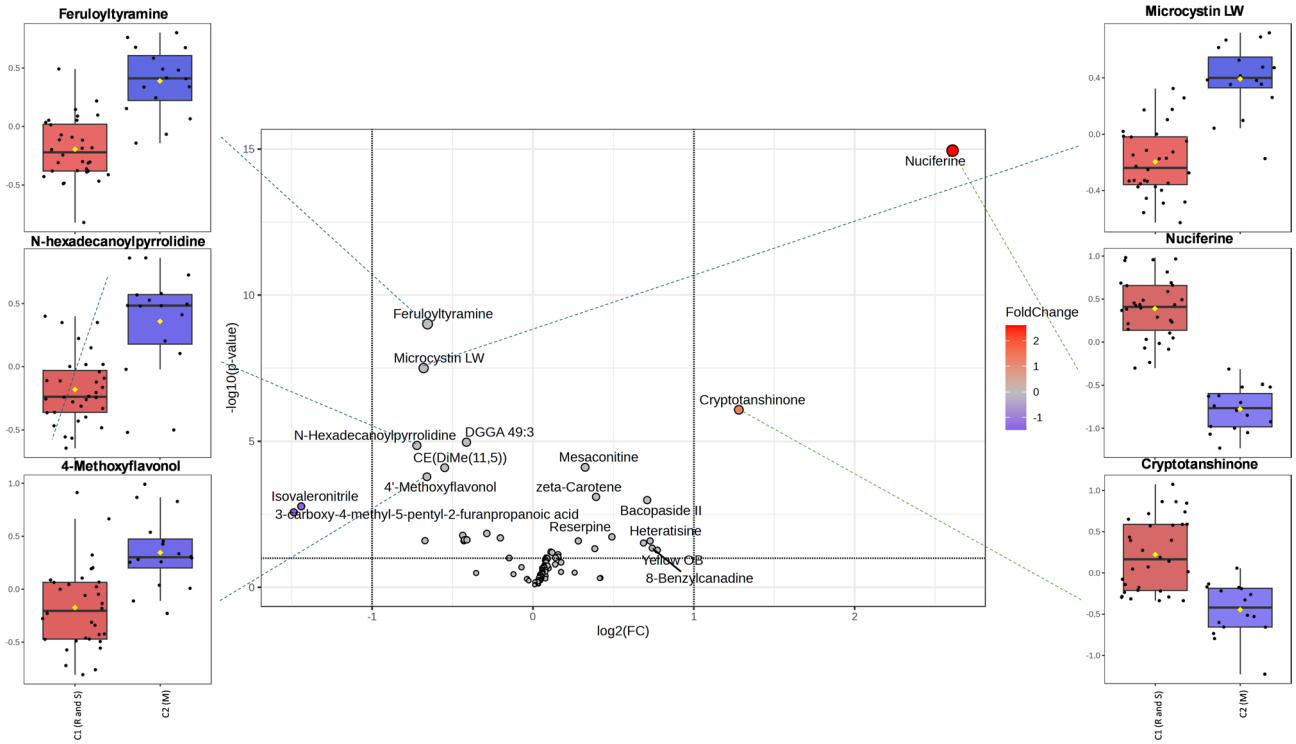

Fig. 4. Volcano plot highlighting differential metabolites between cluster 2 (Marinilla) and cluster 1 (Rionegro and El Santuario).

the lowest p-values, suggesting that the metabolites present in these pathways significantly impact the chemical richness of carrots from the evaluated localities.

Valorization potential of residual carrot biomass based on metabolomic profiles.

The metabolomic analysis revealed a high degree of chemical homogeneity among different morphological types of residual carrot biomass—namely, cracked, deformed, pathologically damaged, and control samples—within each evaluated locality. This consistency indicates that external morphological defects do not significantly alter the metabolic composition of the biomass, supporting the notion that such residues maintain their biochemical integrity and retain substantial potential for Agroindustrial valorization, regardless of their visual quality.

In contrast, metabolomic differentiation was clearly associated with the production locality, reflecting the influence of distinct microclimatic conditions. Samples from Cluster C1 (Rionegro and El Santuario) showed elevated levels of nuciferine and cryptotanshinone, two alkaloids with well-documented pharmacological properties including anti-inflammatory, antioxidant, anticancer, and cardiovascular effects[37–39]. These compounds are considered promising candidates for pharmaceutical and nutraceutical applications (Table 2), and their occurrence under specific climatic patterns suggests potential for targeted agronomic optimization in regions with similar environmental profiles.

Conversely, the Marinilla cluster (C2) exhibited a broader metabolic diversity, with higher relative abundance of 4'-methoxyflavonol, N-hexadecanoylpyrrolidine, feruloyltyramine, and microcystin LW. These metabolites are linked to plant defense mechanisms, stress tolerance, and antioxidant activity[46–56]. Notably, N-hexadecanoylpyrrolidine presents a broad spectrum of bioactivities—including antimicrobial, anticancer, and neuropharmacological effects—making it an attractive molecule for nutraceutical and agrochemical exploration[40–43]. Despite the toxicological concerns associated with microcystin LW[44,45], its detection opens avenues for studying plant–cyanobacteria interactions and assessing potential risks or remediation strategies in agroecosystems. Feruloyltyramine, involved in cell wall reinforcement and abiotic stress response, also underscores the adaptive metabolic responses driven by environmental conditions in high-altitude and high-precipitation zones. These results indicate that microclimate exerts a stronger influence than morphological typology on the metabolomic architecture of residual carrots, and thereby, on their potential applications. This highlights the strategic importance of territoriality in guiding the differentiated valorization of agro-industrial residues. While the identification of bioactive metabolites is promising, the study is constrained by the lack of quantitative metabolite data and absence of validation through analytical standards, which limits immediate industrial scalability; in addition, the observed results should be interpreted with caution, as they did not include negative ionization. Future research should address these limitations through metabolite quantification, standard validation, and bioactivity assays, thus enabling the development of microclimate-specific valorization pathways within the framework of sustainable and circular bioeconomy models.

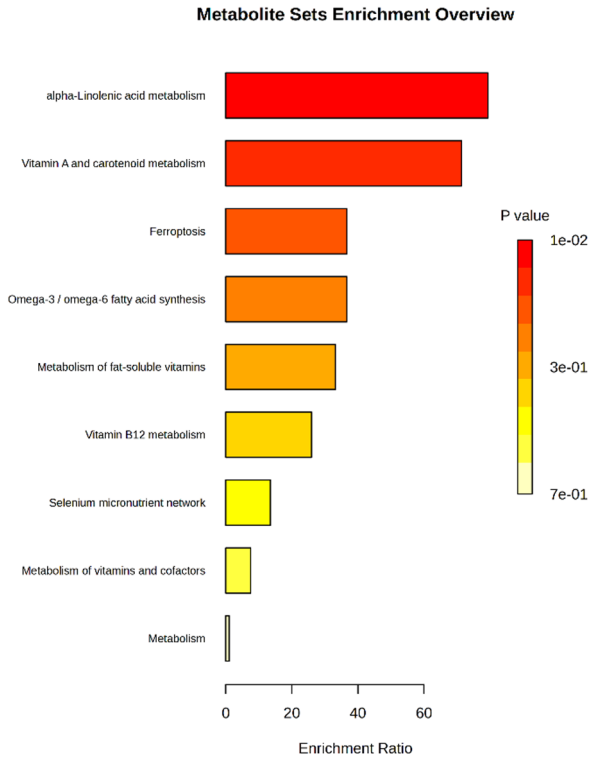

Fig. 5. Metabolomic enrichment analysis of carrot residual biomass samples from the evaluated locations.

Metabolite	Chemical class	Molecular Structure	Relative abundance (normalized intensity)in Cluster	Relevant climate conditions	Potential of bioprospecting
Nuciferine	Diterpene	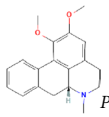 *PubChem CID 10,146*	Abundant in C1 (Rionegro and Santuario)	Warmer temperature, high solar radiation, middle to low altitude.	Bio-functional and nutraceutical foods.
Cryptotanshinone	Alkaloid	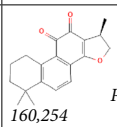 *PubChem CID 160,254*	Abundant in C1 (Rionegro and Santuario)	Warmer temperature, high solar radiation, middle to low altitude.	Medicine treatments (inflammatory, cancer, and cardiovascular protection).
4'-Methoxyflavonol	Flavonoid	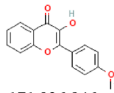 *PubChem CID 171,036,846*	Abundant in C2 (Marinilla)	High precipitation level, high wind speed, high altitude.	Bio-functional and nutraceutical foods.
N-Hexadecanoylpyrrolidine	Alkaloid	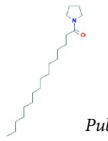 *PubChem CID 247,220*	Abundant in C2 (Marinilla)	High precipitation level, high wind speed, high altitude.	Agrochemical and pharmaceutical industries.
Microcystin LW	Heptapeptide	 *PubChem CID 16,760,564*	Abundant in C2 (Marinilla)	High precipitation level, high wind speed, high altitude.	Bioremediation.
Feruloyltyramine	Phenolamine	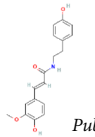 *PubChem CID 5,280,537*	Abundant in C2 (Marinilla)	High precipitation level, high wind speed, high altitude.	Antioxidant product development.

Table 2. Metabolite description and bioprospection potential of Carrot residual biomass.

Discussion

There was no discernible separation between the carrot typologies; however, examining the climate patterns revealed a clear clustering of the three localities. This suggests that pedoclimatic factors and cultural practices exert a greater influence on metabolomic profiles between localities than within each locality[20,52]. Related studies have reported consistent chemical compound contents, such as α-carotene and β-carotene, across different carrot residual types from the same harvest locality[7]. Moreover, geographic origin has been shown to drive metabolomic segregation within the same crop variety[53]. Altitude seems to be an essential factor, as altitude differences can influence local climate conditions, thus affecting the metabolomic variability of agricultural products planted at a specific altitude[15,36,54]. These findings indicate that environmental differences, particularly those influenced by altitude, have a more significant impact on metabolomic variability than the physical or pathological conditions of carrot typologies[16,18,55].

The distinct separation of clusters C1 and C2 based on specific metabolite abundances indicates significant metabolic divergence. This divergence is likely driven by unique environmental factors associated with each cluster, such as altitude, temperature, precipitation, and other climatic characteristics, along with region-specific biotic factors (e.g., the influence of the growth locality), [16,19] which may activate different metabolic pathways, which may then explain variations in chemical composition and bioactive compounds[15,16,19,30]. Additionally, more metabolites were enriched in C2 of Marinilla than in C1 (Rionegro and Santuario). A possible reason for this differential enrichment may be related to the altitude. To adapt to high altitudes, carrot plants may invest more resources in producing secondary metabolites than primary ones[56]; indeed, the secondary metabolite accumulation and the increased activity of antioxidant enzymes are related to a survival strategy for high altitude adaptation[57,58]. Furthermore, distinct climate characteristics such as higher wind speed, precipitation, and cloud cover have been shown to significantly influence the biosynthesis of metabolites in organic waste, aligning with previous findings on the effects of climate on crop quality under abiotic stress[36].

Parallelly, we decided to analyze the biological functions of selected VIPs further. In particular, Nuciferine and Cryptotanshinone had contrasting abundances for both clusters and were higher in C1 than C2. In general, alkaloids, including Nuciferine, exhibit diverse biological activities depending on cellular conditions and receptor interactions, ranging from protective roles to metabolic regulation (e.g., chemical defense or attack) and metabolic regulation[59]. For instance, alkaloids like Nuciferine may be induced in plants under stress conditions and play a protective role against heat and UV light stress[59,60]. Stress-inducing climatic factors, including higher temperatures and greater solar radiation are characteristic of C1 localities, potentially contributing to the enhanced accumulation of Nuciferine in these regions.

Nuciferine is an alkaloid of the aporphine class, previously reported from the lotus plant, that exhibits a broad spectrum of biological activities with significant potential for therapeutic applications. Nuciferine has been associated with activities including anti-hyperlipidemic, anti-obesity, anti-fatty liver, antidiabetic, anti-hyperuricemic, anticancer, anti-inflammatory, antiviral, and antioxidant properties[61]. Additionally, Nuciferine has been linked to promoting longevity, as evidenced by studies in *Caenorhabditis elegans*, where it extended lifespan by approximately 14.86% at a concentration of 100 μM. This effect is attributed to the downregulation of the insulin/IGF-1 signaling pathway, enhancing stress tolerance and overall health[62]. Its anti-inflammatory effects are particularly noteworthy, as Nuciferine modulates oxidative stress and metabolic signaling pathways, playing a crucial role in managing conditions such as obesity, diabetes, and cardiovascular diseases[63]. Cardiovascular protection is another prominent benefit of Nuciferine. By alleviating vascular cell adhesion molecule 1 (VCAM1) activation through autophagy activation and inhibition of the Akt/mTOR signaling pathway, Nuciferine reduces risks associated with cardiovascular events[64]. Moreover, its hepatoprotective effects have been demonstrated in bovine hepatocytes, where it mitigates free fatty acid-induced oxidative damage by activating the TFEB/PGC-1α signaling pathway. This mechanism enhances cellular resilience and decreases oxidative stress markers[65]. Previous findings position Nuciferine as a valuable compound for addressing oxidative damage, metabolic disorders, and inflammatory diseases.

On the other hand, the accumulation of Cryptotanshinone (CPT) in plants appears to be influenced by environmental factors such as radiation, temperature, and precipitation[66,67]. Extreme climatic conditions, including elevated temperatures, intense solar radiation, and high precipitation levels (> 1877 mm), have been associated with increased CPT synthesis[68]. These observations align with the climatic characteristics of higher temperatures and greater solar radiation found in C1 localities. Such conditions likely contribute to the enhanced production of CPT, positioning residual carrots from C1 as a valuable source for bioprospecting and therapeutic exploration. The Cryptotanshinone (CPT), a quinone-diterpene from the tanshinone class, exhibits various biological activities, including antioxidant, anti-inflammatory, cardiovascular protective effects, and potential roles in cancer therapy[69–71]. Its mechanism of action is multifaceted, impacting various cellular processes and signaling pathways critical to its efficacy in diverse applications. In the context of antimicrobial activity, CPT demonstrates significant antibacterial properties by interacting with cell membranes, leading to membrane permeabilization and effectively combating various infectious bacteria[72] In terms of anticancer effects, CPT inhibits the proliferation of melanoma cells by activating the AMPK pathway, which disrupts glycolysis and promotes apoptosis[73]. Additionally, in ovarian cancer, CPT induces metabolic disruption by reducing ATP production and enhancing protein catabolism, resulting in cell cycle arrest[74]. CPT also plays a vital role in metabolic regulation. It has been shown to improve metabolic functions in conditions such as polycystic ovary syndrome (PCOS) by modulating estrogen signaling pathways, which may enhance reproductive health[75]. Moreover, CPT regulates gut microbiota and bile acid metabolism, demonstrating promise in alleviating conditions such as radiation-induced lung fibrosis[76].

In contrast, Marinilla had a larger number of metabolites with VIP scores above 2, such as 4'-Methoxyflavonol, N-Hexadecanoylpyrrolidine, Microcystin LW, and Feruloyltyramine. 4'-Methoxyflavonol belongs to the flavonoid family, which in plants have different functions, mainly as a defense system[77]., a higher flavonoid content has

been associated with higher altitudes[78], which may be related to the higher altitude in Marinilla compared to the other locations and this molecules has been related to antioxidant, anti-acetylcholinesterase, antibacterial, and antifungal activities in halophyte plants[39]. Additionally, 4'-Methoxyflavonol has been used in CO-releasing activities, which benefits the cardiovascular system and inflammation[37,38]. IN-Hexadecanoylpyrrolidine is an N-acylpyrrolidine, as part of pyrrolidine alkaloids (PAs). The PAs are heterocyclic organic compounds synthesized by plants with a wide variety of biological and pharmacological activities, including antioxidant, anti-inflammatory, antibacterial, antifungal, antiparasitic and anthelmintic, anticancer, anti-hyperglycemic, organ protective, and neuropharmacological activities[40,41], and are associated with defense compounds against herbivores and insects[42,43]. The richness of PAs in plant roots has been shown to increase under conditions of higher soil moisture. This suggests that elevated precipitation intensifies pathogenic pressure, thereby enhancing PA synthesis as a defense mechanism against below-ground threats[79]. This phenomenon may explain the higher abundance of N-Hexadecanoylpyrrolidine observed in C2, correlating with the elevated precipitation levels in this locality. While PAs offer exciting opportunities for drug development and agricultural applications, their toxicological profiles necessitate careful evaluation. Balancing their therapeutic benefits against potential risks remains a critical area for future research, aiming to harness their potential safely and effectively.

Additionally, natural pyrrolidine derivatives have been identified in wild carrots[80]. PAs are characterized by their dual nature, offering both therapeutic applications and toxicological concerns. Therapeutically, PAs demonstrate antioxidant properties, effectively mitigating oxidative stress and inflammation; they also exhibit antimicrobial activity, making them promising candidates for antibacterial and antifungal treatments[40]. Furthermore, some PAs show anticancer potential, with mechanisms involving cell cycle regulation and apoptosis induction[40,81].

However, PAs are not without risks. Toxicological concerns include hepatotoxicity, where specific compounds are linked to liver damage and hepatocarcinogenesis[81,82]. Neurotoxicity has also been observed, as PAs can antagonize muscarinic acetylcholine receptors, leading to adverse effects on the nervous system[83]. Additionally, PAs have been associated with genotoxic effects, such as DNA damage and cell cycle disruptions, raising concerns about their mutagenic potential[81]. Microcystin LW belongs to the microcystin family, a family of cyclic heptapeptides produced and released to the surface water of lakes and reservoirs during cyanobacterial blooms[44,45]. Some climatic conditions related to severe storms and rainfall events, rising CO_2 concentrations, global climate change, or eutrophic water conditions contribute to this occurrence[45,84]. Root vegetable crops like carrots may act as an exposure medium when they are irrigated with water containing cyanobacteria. The cyanobacteria cell may stick to plant tissues, and therefore microcystins can be absorbed[84,85]. Great precipitations and agricultural practices possibly related to irrigation water systems and reservoir water used in C2 could influence the presence of Microcystin LW in those residual biomass carrots. Microcystin LW is a potent biological toxin with diverse effects on living organisms, extending beyond its well-known hepatotoxicity to include neurotoxic and ecotoxicological impacts. Hepatotoxicity remains its most recognized effect, as Microcystin LW disrupts liver function, inducing hepatocyte cell death. Long-term exposure to contaminated water can result in severe liver damage in both humans and animals[86,87]. Neurotoxic effects have also been observed, with studies indicating selective cytotoxicity in rat astrocytes, leading to reduced cell viability and increased apoptosis[44]. Furthermore, the toxin disrupts cytoskeletal integrity in astrocytes, compromising homeostasis critical for proper brain function[44].

Ecologically, Microcystin LW poses significant risks as it accumulates in aquatic organisms and can enter the food chain, impacting higher trophic levels, including humans[86]. Its presence in agricultural systems, such as through contaminated irrigation water, can also negatively affect crops, resulting in broader ecological consequences[86]. These findings underscore the importance of monitoring and managing water sources used for irrigation, particularly in regions like C2, where high precipitation levels may exacerbate cyanobacterial contamination and toxin absorption in crops.

Feruloyltyramine is a phenolamine reported as a polyphenol compound with antioxidant activity[88,89]. Phenolamines are secondary metabolites which are derived from the conjugation of a phenolic fraction with polyamines. Their function in plants is related to cell wall reinforcement and defense through toxicity for pathogens and predators[90,91]. Polyamines, in general, have a role in developing stress tolerance, including resistance to salt, high and low temperatures, hypoxia, hyperosmosis, and atmospheric pollutants[91]. Local climatic characteristics may increase abiotic stress conditions in C2, considering the greater altitude, precipitation, and higher wind speed, which may mediate Feruloyltyramine production. Beyond its role in plants, N-trans-feruloyltyramine (NTF), a derivative of Feruloyltyramine, exhibits a range of biological activities, including neuroprotection, antioxidant effects, and anti-inflammatory properties. Research indicates that NTF can mitigate cholinergic dysfunction and memory impairment, particularly in neurodegeneration models such as scopolamine-induced cognitive decline in rats[92]. This neuroprotective effect involves the reduction of reactive oxygen species (ROS) and apoptosis markers in brain tissues[92]. NTF also demonstrates significant antioxidant capabilities by lowering intracellular ROS levels in neuroblastoma cells. It reverses H_2O_2-induced apoptosis through modulation of pro-apoptotic and anti-apoptotic proteins, highlighting its cytoprotective potential[93]. Additionally, NTF exhibits anti-inflammatory mechanisms by suppressing inflammatory mediators such as iNOS and COX-2 in macrophages through the inhibition of AP-1 and MAPK signaling pathways[94]. While the therapeutic potential of NTF is promising, further studies are needed to explore its full pharmacological profiles and safety in clinical applications. The interplay between local abiotic stress factors in C2 and the enrichment of Feruloyltyramine underscores its potential as a source of bioactive compounds. These findings suggest that climatic factors could drive the production of metabolites like Feruloyltyramine with significant applications in neuroprotection, antioxidant therapies, and inflammation management.

Some studies conducted on the carrot metabolome have revealed a similar number of annotated metabolites, with very few works focusing on the evaluation of the direct effects of locality or microclimate on the metabolome,

reporting annotations of up to 86 metabolites, which include organic acids, phenolic compounds, carotenoids, among others[29,30], but none of the aforementioned. Other studies have particularly focused on analyzing the richness in terpenes as an impact on the flavor of carrots[95], or the effect of different production systems or simple transformation processes[96,97]; However, so far, no study has been reported that focuses its efforts on the effect of the microclimate associated with the harvesting locality on the residual biomass of carrots.

The α-linolenic acid metabolism involved in unsaturated fatty acid biosynthesis has been reported to exhibit particular enrichment under cold or low-temperature stress and reduced water availability[98,99]. This pathway, which includes oleic acid and linoleic acid, serves as a gateway to the biosynthesis of various unsaturated fatty acids[99], and is closely linked to antioxidant production and jasmonic acid biosynthesis[98]. On the other hand, high levels of atmospheric humidity and greater precipitations have varying effects on carotenoid accumulation, with a negative impact on β-carotene content and a positive effect on α-branch carotenoid and total carotenoids, respectively. Additionally, photoperiod and light intensity duration have been reported as a differential factor on α-branch or β-branch carotenoid biosynthesis, with high radiation duration and photoperiod having a more significant positive effect on α-branch carotenoid accumulation, while exposure to low light intensity increases β-carotene content[52].

Other pathways, such as ferroptosis, iron-dependent programmed cell death, and omega-3/omega-6 fatty acid synthesis, also showed considerable enrichment. Ferroptosis, such as an iron-dependent, oxidative cell death process, has a physiological role in cell death regulation in response to heat stress in plants[100,101]; moreover, cellular susceptibility to ferroptosis is significantly influenced by the polyunsaturated fatty acids absorption and metabolism, and synthesis of polyunsaturated fatty acids-phospholipids[102], being linolenic acid, the primary polyunsaturated fatty acids obtained from plant food sources[100]. Other pathways with lower significance levels, such as those related to vitamin and micronutrient metabolism, are also statistically relevant. For instance, the alpha-tocopherol role in ferroptosis inhibition is the typical endogenous lipophilic radical-trapping antioxidant[102]. This result suggests that there may also be differential regulation of these pathways, albeit with less impact on the observed differences.

The physiological adaptability of plants to their local microclimates aligns with the capacity of certain plants to modify biosynthetic pathways of secondary compounds such as polyphenols and terpenoids, adapting to environmental variations through a process known as phenotypic plasticity. This plasticity enables plants to maintain stability and synthesize bioactive compounds with antioxidant and nutraceutical properties[103,104]. More remarkably, plasticity has been primarily noted for terpene molecules and phenolic compounds (Myristicin, 6-methoxymellein, and D-germacrene) in different carrot varieties and locations, suggesting a co-regulation mechanism in their accumulation, which indicates that these compounds appear to have a similar pattern with common localities and varieties implicated in accumulation[29].

Moreover, the enriched metabolic pathways offer significant opportunities for bioprospecting, mainly through α-linolenic acid metabolism, carotenoid biosynthesis, ferroptosis, and omega-3/omega-6 fatty acid synthesis. The α-linolenic acid pathway plays a central role in the biosynthesis of unsaturated fatty acids, which are precursors for antioxidant compounds[98,99]. This pathway could be explored to develop bio-functional or nutraceutical products based on carrot residual biomass. Carotenoid biosynthesis, influenced by environmental factors such as light intensity and humidity, has potential in biofortification programs that optimize α- and β-carotenoid levels in carrot crops[52]. This potential is particularly relevant for improving dietary vitamin A intake and antioxidant activity under varying agroclimatic conditions. The ferroptosis pathway, mediated by iron-dependent oxidative stress, allows studying stress-induced cell death mechanisms in carrot plants. Its interplay with polyunsaturated fatty acid metabolism and the role of alpha-tocopherol as an endogenous ferroptosis inhibitor highlight its potential in developing biotechnological tools to enhance stress tolerance and crop resilience[100,102]. Finally, the omega-3/omega-6 fatty acid synthesis pathway underscores its importance in using carrot residual biomass to produce essential fatty acids for human health. Together with micronutrient metabolism, these pathways could serve as key targets for agricultural, nutraceutical, and pharmaceutical applications, supporting sustainable crop production and human nutrition.

Conclusion

This study underscores the significant impact of agroclimatic conditions on the metabolomic profiles of residual carrot biomass from three Colombian localities. The metabolomic differences between clusters C1 (Rionegro and El Santuario) and C2 (Marinilla) highlight the influence of environmental factors such as altitude, precipitation, temperature, and solar radiation in shaping metabolic profiles. Notably, metabolites like Nuciferine and Cryptotanshinone were more abundant in C1, consistent with the warmer temperatures and higher solar radiation in these localities. Conversely, metabolites such as 4′-methoxyflavonol, N-Hexadecanoylpyrrolidine, Microcystin LW, and Feruloyltyramine were enriched in C2, correlating with Marinilla's higher altitude and precipitation levels.

The bioprospecting potential of these metabolites is substantial. Compounds such as Nuciferine and Cryptotanshinone show promise for pharmaceutical and nutraceutical applications due to their antioxidant, anti-inflammatory, and anticancer properties. Similarly, metabolites enriched in C2, including 4′-methoxyflavonol and N-Hexadecanoylpyrrolidine, hold potential for use in functional foods and agrochemical innovations. Pathways like α-linolenic acid metabolism and carotenoid biosynthesis further highlight the potential of residual carrots as a sustainable resource for producing bioactive compounds. However, a future research phase is necessary to further validate with reference standards and quantify the metabolites identified, thereby providing a more comprehensive understanding of the metabolomic profiles and their potential applications or precautions. Additionally, metabolomic studies (not lipidomic) are recommended to achieve a deeper understanding of the differences in carrot biomass typologies.

These findings advance the valorization of agricultural waste, offering a foundation for future biotechnological and agricultural innovations; moreover, this study is pioneering in evaluating the effects of microclimate on carrot residual biomass associated with the harvest location. By optimizing the use of residual biomass through targeted bioprospecting, this research bridges the gap between food waste management and the development of high-value bio-based products. This approach supports circular economy models, promoting environmental sustainability while driving economic growth.

The supplementary data can be found in Mendeley Data online ("Carrot residual biomass supplementary metabolomic data", Mendeley Data, V1, https://data.mendeley.com/datasets/7vbbkv6n9t/2).

Acknowledgements.

Data availability

The supplementary data can be found in Mendeley Data online ("Carrot residual biomass supplementary metabolomic data", Mendeley Data, V2, https://data.mendeley.com/datasets/7vbbkv6n9t/2).The raw LC–MS data (.mzxl files) and processed outputs are available in Metabollights public repository, with accession number: MTBLS20251010213740 (https://www.ebi.ac.uk/metabolights/editor/study/MTBLS20251010213740).

Received: 13 March 2025; Accepted: 19 January 2026
Published online: 10 February 2026

References

1. Ahmad, T. et al. Phytochemicals in daucus carota and their health benefits—review article. *Foods* vol. 8 Preprint at (2019). https://doi.org/10.3390/FOODS8090424
2. Que, F. et al. Advances in research on the carrot, an important root vegetable in the Apiaceae family. *Horticulture Research* vol. 6 Preprint at (2019). https://doi.org/10.1038/s41438-019-0150-6
3. Rodrigues, J. P. B. et al. Agri-Food Surplus, Waste and Loss as Sustainable Biobased Ingredients: A Review. *Molecules* vol. 27 Preprint at (2022). https://doi.org/10.3390/molecules27165200
4. FAOSTAT. *Cultivos y productos de ganadería* (2023). https://www.fao.org/faostat/es/#data
5. Ministerio de Agricultura y Desarrollo Rural. *Sector Agrícola Colombiano – 2015*. (2015). https://sioc.minagricultura.gov.co/Hortalizas/Documentos/2015-07-30%20Cifras%20Sectoriales.pdf
6. Chauhan, C., Dhir, A., Akram, M. U. & Salo, J. Food loss and waste in food supply chains. A systematic literature review and framework development approach. *J. Clean. Prod.* **295**, 126438 (2021).
7. Jyot Kaur, G., Kumar, D., Orsat, V. & Singh, A. Assessment of Carrot rejects and wastes for food product development and as a biofuel. *Biomass Convers. Biorefin.* **12**, 757–768 (2020).
8. Vaz, A., Odriozola-Serrano, A. & Oms-Oliu, I. G. & Martín-Belloso, O. Physicochemical Properties and Bioaccessibility of Phenolic Compounds of Dietary Fibre Concentrates from Vegetable By-Products. *Foods* 11, (2022).
9. Eliopoulos, C., Markou, G., Langousi, I. & Arapoglou, D. Reintegration of Food Industry By-Products: Potential Applications. *Foods* vol. 11 Preprint at (2022). https://doi.org/10.3390/foods11223743
10. Cámara de comercio de Bogotá. Manual Zanahoria. (2015).
11. ICONTEC. Norma técnica colombiana NTC 1226: Frutas y hortalizas frescas: Zanahoria. (1994). https://ecollection-icontec-org.ezproxy.unal.edu.co/normavw.aspx?ID=538
12. Ramos-Andrés, M., Aguilera-Torre, B. & García-Serna, J. Biorefinery of discarded Carrot juice to produce carotenoids and fermentation products. *J. Clean. Prod.* **323**, 129139 (2021).
13. Salvañal, L., Clementz, A., Guerra, L., Yori, J. C. & Romanini D. l-lactic acid production using the syrup obtained in biorefinery of Carrot discards. *Food Bioprod. Process.* **127**, 465–471 (2021).
14. Vigneshwar, S. S. et al. Bioprocessing of Biowaste derived from food supply chain side-streams for extraction of value added bioproducts through biorefinery approach. *Food Chem. Toxicol.* **165**, 113184 (2022).
15. Večeřová, K. et al. Single and interactive effects of variables associated with climate change on wheat metabolome. *Front. Plant. Sci.* **13**, 1002561 (2022).
16. Chelghoum, M. et al. Influence of altitude, precipitation, and temperature factors on the phytoconstituents, antioxidant, and α-amylase inhibitory activities of pistacia Atlantica. *J. Food Meas. Charact.* **15**, 4411–4425 (2021).
17. Kecis, H. et al. Phenolic profile and bioactivity of the aerial part and roots of mentha rotundifolia L. grown in two different localities in Northeastern algeria: A comparative study. *Biocatal. Agric. Biotechnol.* **47**, 102581 (2023).
18. Zhao, Z. et al. Altitudinal variation of Dragon fruit metabolite profiles as revealed by UPLC-MS/MS-based widely targeted metabolomics analysis. *BMC Plant. Biol.* **24**, 1–12 (2024).
19. Brahmi, F. et al. Impact of growth sites on the phenolic contents and antioxidant activities of three Algerian mentha species (M. pulegium L., M. rotundifolia (L.) Huds., and M. spicata L). *Front. Pharmacol.* **13**, 886337 (2022).
20. Cornara, L. et al. Pedoclimatic Conditions Influence the Morphological, Phytochemical and Biological Features of Mentha pulegium L. *Plants* 12, 24 (2023).
21. Tiwari, S., Yawale, P., Upadhyay, N. & Carotenoids Extraction strategies and potential applications for valorization of under-utilized waste biomass. *Food Bioscience* **48,** 101812 (2022).
22. Idrovo Encalada, A. M. et al. High-power ultrasound pretreatment for efficient extraction of fractions enriched in pectins and antioxidants from discarded carrots (Daucus Carota L). *J. Food Eng.* **256**, 28–36 (2019).
23. Fukusaki, E. Application of Metabolomics for High-Resolution Phenotype Analysis. *Rinsho byori. The Japanese journal of clinical pathology* vol. 63 736–745 Preprint at (2015). https://doi.org/10.5702/massspectrometry.s0045
24. Viant, M. R., Kurland, I. J., Jones, M. R. & Dunn, W. B. How close are we to complete annotation of metabolomes? *Curr. Opin. Chem. Biol.* **36**, 64–69 (2017).
25. Sutliff, A. K. et al. Lipidomics-based comparison of molecular compositions of green, yellow, and red bell peppers. *Metabolites* 11, (2021).
26. Hoffmann, J. F., Carvalho, I. R., Barbieri, R. L., Rombaldi, C. V. & Chaves, F. C. Butia spp. (Arecaceae) LC-MS-based metabolomics for species and geographical origin discrimination. *J. Agric. Food Chem.* **65**, 523–532 (2017).
27. Luque de Castro, M. D., Quiles-Zafra, R. & Lipidomics An omics discipline with a key role in nutrition. *Talanta* **219**, 121197 (2020).
28. Stra, A., Almarwaey, L. O., Alagoz, Y., Moreno, J. C. & Al-Babili, S. Carotenoid metabolism: new insights and synthetic approaches. *Front Plant. Sci* **13**, 1072061 (2023).
29. Chevalier, W. et al. Multisite evaluation of phenotypic plasticity for specialized metabolites, some involved in Carrot quality and disease resistance. *PLoS One.* **16**, e0249613 (2021).

30. Koudela, M. et al. Effect of agroecological conditions on biologically active compounds and metabolome in carrot. *Cells* 10, (2021).
31. Peterson, A. Townsend. Ecological niches and geographic distributions. *Climatic data collection* (2017).
32. Henao-Rojas, J. C. et al. Towards bioprospection of commercial materials of mentha spicata L. Using a combined strategy of metabolomics and biological activity analyses. *Molecules* **27**, 3559 (2022).
33. Kanehisa, M., Furumichi, M., Sato, Y. & Kawashima, M. Ishiguro-Watanabe, M. KEGG for taxonomy-based analysis of pathways and genomes. *Nucleic Acids Res.* **51**, D587–D592 (2023).
34. Kanehisa, M. Toward understanding the origin and evolution of cellular organisms. *Protein Science* vol. 28 1947– Preprint at (1951). https://doi.org/10.1002/pro.3715 (2019).
35. Kanehisa, M. & Goto, S. *KEGG: Kyoto encyclopedia of genes and genomes. Nucleic Acids Research* **28,** 27-30 (2000). http://www.genome.ad.jp/kegg/
36. Romero, H., Pott, D. M., Vallarino, J. G. & Osorio, S. Metabolomics-Based Evaluation of Crop Quality Changes as a Consequence of Climate Change. *Metabolites* 11, (2021).
37. Han, X., Whitfield, S. & Cotten, J. Synthesis, characterization and CO-releasing property of palladium(II) bipyridine flavonolate complexes. *Transition Met. Chem.* **45**, 217–225 (2020).
38. Su, Y., Yang, W., Yang, X., Zhang, R. & Zhao, J. Visible Light-Induced CO-Release reactivity of a series of ZnII–Flavonolate complexes. *Aust J. Chem.* **71**, 549–558 (2018).
39. Stanković, M. & Jakovljević, D. Phytochemical diversity of halophytes. *Handb. Halophytes: Molecules Ecosyst. Towards Biosaline Agric.* **2089-2114** https://doi.org/10.1007/978-3-030-57635-6_125 (2021).
40. Islam, M. T. & Mubarak, M. S. Pyrrolidine alkaloids and their promises in pharmacotherapy. *Adv. Traditional Med.* **20**, 13–22 (2020).
41. Poyraz, S., Döndaş, H. A., Döndaş, N. Y. & Sansano, J. M. Recent insights about pyrrolidine core skeletons in Pharmacology. *Front. Pharmacol.* **14**, 1239658 (2023).
42. Schramm, S., Köhler, N. & Rozhon, W. Pyrrolizidine alkaloids: Biosynthesis, biological activities and occurrence in crop plants. *Molecules* **24**, 498 (2019).
43. Srivasatava, P. Use of alkaloids in plant protection. *Plant. Protection: Chemicals Biol.* 337–351. https://doi.org/10.1515/9783110771558-013/HTML (2022).
44. Bulc Rozman, K., Jurič, D. M. & Šuput, D. Selective cytotoxicity of microcystins LR, LW and LF in rat astrocytes. *Toxicol. Lett.* **265**, 1–8 (2017).
45. Levizou, E., Papadimitriou, T., Papavasileiou, E., Papadimitriou, N. & Kormas, K. A. Root vegetables bioaccumulate microcystins-LR in a developmental stage-dependent manner under realistic exposure scenario: the case of Carrot and radish. *Agric. Water Manag.* **240**, 106274 (2020).
46. Nuciferine | C19H21NO2 | CID 10146. - PubChem. https://pubchem.ncbi.nlm.nih.gov/compound/Nuciferine#section=2D-Structure
47. Cryptotanshinone | C19H20O3 | CID 160254. - PubChem. https://pubchem.ncbi.nlm.nih.gov/compound/160254#section=2D-Structure
48. 3-Hydroxy-4'-methoxyflavone. (4'-Methoxyflavonol) | C32H24O8 | CID 171036846 - PubChem. https://pubchem.ncbi.nlm.nih.gov/compound/171036846#section=2D-Structure
49. 1-Hexadecanoylpyrrolidine | C20H39NO | CID. 247220 - PubChem. https://pubchem.ncbi.nlm.nih.gov/compound/247220#section=2D-Structure
50. MC-LW | C54H72N8O12 | CID. 16760564 - PubChem. https://pubchem.ncbi.nlm.nih.gov/compound/16760564#section=2D-Structure
51. N-Trans-feruloyltramine | C18H19NO4 | CID. 5280537 - PubChem. https://pubchem.ncbi.nlm.nih.gov/compound/5280537#section=2D-Structure
52. Chevalier, W. et al. Evaluation of pedoclimatic factors and cultural practices effects on carotenoid and sugar content in Carrot root. *Eur. J. Agron.* **140**, 126577 (2022).
53. El-Shabasy, R. M. et al. Valorization potential of Egyptian mango kernel waste product as analyzed via GC/MS metabolites profiling from different cultivars and geographical origins. *Scientific Reports 2024 14:1* 14, 1–14 (2024).
54. Almeida, J., Perez-Fons, L. & Fraser, P. D. A transcriptomic, metabolomic and cellular approach to the physiological adaptation of tomato fruit to high temperature. *Plant. Cell. Environ.* **44**, 2211–2229 (2021).
55. Lu, A. et al. UPLC-Q/TOF-MS coupled with multivariate analysis for comparative analysis of metabolomic in dendrobium nobile from different growth altitudes. *Arab. J. Chem.* **15**, 104208 (2022).
56. Pan, L. et al. Altitudinal variation on Metabolites, Elements, and antioxidant activities of medicinal plant Asarum. *Metabolites* **13**, 1193 (2023).
57. Ibrahim, I. A. et al. Adaptive responses of four medicinal plants to high altitude oxidative stresses through the regulation of antioxidants and secondary metabolites. *Agron. 2022.* **12, Page 3032** (12), 3032 (2022).
58. Hashim, A. M. et al. Oxidative stress responses of some endemic plants to high altitudes by intensifying antioxidants and secondary metabolites content. *Plants 2020.* **9**, 869 (2020).
59. Aniszewski, T. Elsevier,. Biology of alkaloids. in *Alkaloids* 195–258 (2015). https://doi.org/10.1016/B978-0-444-59433-4.00003-1
60. Yazaki, K. ABC transporters involved in the transport of plant secondary metabolites. *FEBS Lett.* **580**, 1183–1191 (2006).
61. Huang, X., Hao, N., Chen, G., Liu, S. & Che, Z. Chemistry and biology of Nuciferine. *Ind. Crops Prod.* **179**, 114694 (2022).
62. Xu, Y., Miao, Y. & Li, R. Nuciferine Promotes Longevity and Fitness in Caenorhabditis elegans through the Regulation of the Insulin/IGF-1 Signaling Pathway. *J Food Biochem* 2779989 (2024). (2024).
63. Zhao, T. et al. Structure-activity relationship, bioactivities, molecular mechanisms, and clinical application of Nuciferine on inflammation-related diseases. *Pharmacol. Res.* **193**, 106820 (2023).
64. Wei, H. et al. Nuciferine induces autophagy to relieve vascular cell adhesion molecule 1 activation via repressing the Akt/mTOR/AP1 signal pathway in the vascular endothelium. *Front. Pharmacol.* **14**, 1264324 (2023).
65. Fang, Z. et al. Nuciferine protects bovine hepatocytes against free fatty acid-induced oxidative damage by activating the transcription factor EB/peroxisome proliferator-activated receptor γ coactivator 1 alpha pathway. *J. Dairy. Sci.* **107**, 625–640 (2024).
66. He, C. E., Wei, J., Jin, Y. & Chen, S. Bioactive components of the roots of salvia miltiorrhizae: changes related to harvest time and germplasm line. *Ind. Crops Prod.* **32**, 313–317 (2010).
67. He, C. et al. Deciphering the effects of genotype and Climatic factors on the performance, active ingredients and rhizosphere soil properties of salvia miltiorrhiza. *Front. Plant. Sci.* **14**, 1110860 (2023).
68. Zhang, C. et al. Correlation analysis between meteorological factors, biomass, and active components of salvia miltiorrhiza in different Climatic zones. *Zhongguo Zhong Yao Za Zhi.* **40**, 607–613 (2015).
69. Zhu, J. et al. An overview of chemical inhibitors of the Nrf2-ARE signaling pathway and their potential applications in cancer therapy. *Free Radic Biol. Med.* **99**, 544–556 (2016).
70. Xing, Z., Bi, G., Li, T., Zhang, Q. & Knight, P. R. Effect of harvest time on growth and bioactive compounds in salvia miltiorrhiza. *Plants* **13**, 1788 (2024).
71. Wei, F. et al. Natural products and mitochondrial allies in colorectal cancer therapy. *Biomed. Pharmacother.* **167**, 115473 (2023).

72. Ortiz, J., Aranda, F. J., Teruel, J. A. & Ortiz, A. Cryptotanshinone-Induced permeabilization of model phospholipid membranes: A biophysical study. *Membr. 2024.* **14**, 118 (2024).
73. Chen, Q. et al. Cryptotanshinone inhibits PFK-mediated aerobic Glycolysis by activating AMPK pathway leading to Blockade of cutaneous melanoma. *Chin. Med. (United Kingdom).* **19**, 1–14 (2024).
74. Wang, T. et al. Study on the intervention mechanism of Cryptotanshinone on human A2780 ovarian cancer cell line using GC-MS-Based cellular metabolomics. *Pharmaceuticals 2023.* **16**, 861 (2023).
75. Liu, Y. C. et al. Mechanism of Cryptotanshinone to improve endocrine and metabolic functions in the endometrium of PCOS rats. *J. Ethnopharmacol.* **319**, 117346 (2024).
76. Li, Z. et al. Cryptotanshinone alleviates radiation-induced lung fibrosis via modulation of gut microbiota and bile acid metabolism. *Phytother. Res.* **37**, 4557–4571 (2023).
77. Do, S. et al. Flavonols and Flavones as Potential anti-Inflammatory, Antioxidant, and Antibacterial Compounds. *Oxid Med Cell Longev* 9966750 (2022). (2022).
78. Wu, X. & Xiao, J. Response and adaptive mechanism of flavonoids in pigmented potatoes at different altitudes. *Plant. Cell. Physiol.* **65**, 1184–1196 (2024).
79. Kirk, H., Vrieling, K., van der Meijden, E. & Klinkhamer, P. G. L. Species by environment interactions affect pyrrolizidine alkaloid expression in senecio jacobaea, senecio aquaticus, and their hybrids. *J. Chem. Ecol.* **36**, 378–387 (2010).
80. Boshra, Y. R., Mostafa, Y. A., Hamed, A. N. E., Desoukey, S. Y. & Fahim, J. R. Wound healing potential of narcissus pseudonarcissus L. bulbs supported with chemical and molecular Docking investigations. *South. Afr. J. Bot.* **157**, 490–501 (2023).
81. Abdelfatah, S. et al. Pyrrolizidine alkaloids cause cell cycle and DNA damage repair defects as analyzed by transcriptomics in cytochrome P450 3A4-overexpressing HepG2 clone 9 cells. *Cell. Biol. Toxicol.* **38**, 325–345 (2022).
82. Wei, X., Ruan, W. & Vrieling, K. Current Knowledge and Perspectives of Pyrrolizidine Alkaloids in Pharmacological Applications: A Mini-Review. *Molecules 2021, Vol. 26, Page 1970* 26, (2021). (1970).
83. Abdalfattah, S. et al. Identification of antagonistic action of pyrrolizidine alkaloids in muscarinic acetylcholine receptor M1 by computational target prediction analysis. *Pharmaceuticals 2024.* **17**, 80 (2024).
84. Drobac Backović, D. & Tokodi, N. Cyanotoxins in food: exposure assessment and health impact. *Food Res. Int.* **184**, 114271 (2024).
85. Van Hassel, W. H. R., Masquelier, J., Andjelkovic, M. & Rajkovic, A. Towards a better quantification of cyanotoxins in fruits and vegetables: validation and application of an UHPLC-MS/MS-Based method on Belgian products. *Separations* **9**, 319 (2022).
86. Kh. Kelini, W., Mahmoud, M. A. M., Zaky, Z. M. & Abdel-Mohsein, H. S. Toxicity of microcystins on human, animal and aquatic life. *Int. J. Compr. Veterinary Res.* **1**, 1–13 (2023).
87. Wei, N., Hu, C., Dittmann, E. & Song, L. Gan, N. The biological functions of microcystins. *Water Res.* **262**, 122119 (2024).
88. Forino, M., Tartaglione, L., Dell'Aversano, C. & Ciminiello, P. NMR-based identification of the phenolic profile of fruits of lycium barbarum (goji berries). Isolation and structural determination of a novel N-feruloyl tyramine dimer as the most abundant antioxidant polyphenol of Goji berries. *Food Chem.* **194**, 1254–1259 (2016).
89. Li, W. J. et al. Phenolic compounds and antioxidant activities of liriope muscari. *Molecules 2012.* **17**, 1797–1808 (2012).
90. Grandmaison, J., Olah, G. M., Van Calsteren, M. R. & Furlan, V. Characterization and localization of plant phenolics likely involved in the pathogen resistance expressed by endomycorrhizal roots. *Mycorrhiza* **3**, 155–164 (1993).
91. Gupta, K., Dey, A. & Gupta, B. Plant polyamines in abiotic stress responses. *Acta Physiologiae Plantarum 2013 35:7* 35, 2015–2036 (2013).
92. Thangnipon, W. et al. Protective roles of N-trans-feruloyltyramine against Scopolamine-Induced cholinergic dysfunction on cortex and hippocampus of rat brains. *Siriraj Med. J.* **73**, 413–422 (2021).
93. Soi-ampornkul, R. et al. N-trans-feruloyltyramine protects human neuroblastoma SK-N-SH cell line against H2O2-Induced cytotoxicity. *Nat Prod. Commun* **17**, 1-8 (2022).
94. Jiang, Y., Yu, L. & Wang, M. H. N-trans-feruloyltyramine inhibits LPS-induced NO and PGE2 production in RAW 264.7 macrophages: involvement of AP-1 and MAP kinase signalling pathways. *Chem. Biol. Interact.* **235**, 56–62 (2015).
95. Qi, X. Y., Kong, X. P., Zhou, H. W. & Yan, X. P. Crucial factors impacting Carrot flavor analysis based on broad target metabolomics. *Scientia Agricultura Sinica*. **57**, 3250–3263 (2024).
96. Zhou, N., Ma, S., Zhang, M. & Wang, J. Effects of different cutting styles on physiological properties in Fresh-Cut carrots. *Plants 2024.* **13**, 1665 (2024).
97. Schulzova, V., Koudela, M., Chmelarova, H., Hajslova, J. & Novotny, C. Assessment of Carrot Production System Using Biologically Active Compounds and Metabolomic Fingerprints. *Agronomy* Vol. 12, Page 1770 12, 1770 (2022). (2022).
98. Zi, X., Zhou, S. & Wu, B. Alpha-Linolenic acid mediates diverse drought responses in maize (Zea Mays L.) at seedling and flowering stages. *Molecules* **27**, 771 (2022).
99. Liu, W. et al. Transcriptomic and physiological analysis reveal that α-Linolenic acid biosynthesis responds to early chilling tolerance in pumpkin rootstock varieties. *Front. Plant. Sci.* **12**, 669565 (2021).
100. Liang, D., Minikes, A. M. & Jiang, X. Ferroptosis at the intersection of lipid metabolism and cellular signaling. *Mol. Cell.* **82**, 2215–2227 (2022).
101. Distéfano, A. M. et al. Heat stress induces ferroptosis-like cell death in plants. *J. Cell Biol.* **216**, 463–476 (2017).
102. Pope, L. E. & Dixon, S. J. Regulation of ferroptosis by lipid metabolism. *Trends Cell. Biol.* **33**, 1077–1087 (2023).
103. Savoi, S. et al. Transcriptome and metabolite profiling reveals that prolonged drought modulates the phenylpropanoid and terpenoid pathway in white grapes (Vitis vinifera L). *BMC Plant. Biol* **16**, 67-84 (2016).
104. Pott, D. M., Osorio, S. & Vallarino, J. G. From central to specialized metabolism: an overview of some secondary compounds derived from the primary metabolism for their role in conferring nutritional and organoleptic characteristics to fruit. *Front. Plant. Sci.* **10**, 454686 (2019).

Acknowledgements

The authors thank the Science, Technology, and Innovation Fund of the General Royalties System (SGR) of Colombia for funding this research, through the project called: "Fortalecimiento de la cadena productiva de la zanahoria mediante la creación de prototipos de productos innovadores en el Oriente del departamento de Antioquia" (code BPIN: 2020000100192). Also, we thank the Colombian Agricultural Research Corporation—Agrosavia, the National University of Colombia, and the National Learning Service — SENA, for the time dedicated by the researchers and the use of the assets inherent in preparing this document.

The authors thank the Science, Technology, and Innovation Fund of the General Royalties System (SGR) of Colombia for funding this research, through the project called: "*Fortalecimiento de la cadena productiva de la zanahoria mediante la creación de prototipos de productos innovadores en el Oriente del departamento de Antioquia*" (code BPIN: 2020000100192). Also, we thank the Colombian Agricultural Research Corporation-Agrosavia, the National University of Colombia, and the National Learning Service — SENA, for the time dedicated by the researchers and the use of the assets inherent in preparing this document.

Author contributions

JM-S, JCH-R, AG, LFL-H, EMC-C and DPY-B: conceptualization; JM-S, JCH-R, AG and LFL-H: methodology; JM-S, JCH-R, EMC-C and DPY-B: formal analysis; JM-S, JCH-R, AG and LFL-H: investigation; JCH-R, AG and LFL-H: data curation; JM-S, JCH-R, AG, LFL-H, EMC-C and DPY-B: writing - original draft; JCH-R, EMC-C and DPY-B: writing - review & editing; JM-S and AG: visualization; JCH-R, AG, LFL-H, EMC-C and DPY-B: supervision; JCH-R: project administration; JM-S, JCH-R, AG, LFL-H, EMC-C and DPY-B: funding acquisition. All authors have read and agreed to the published version of the manuscript.

Funding

This research was funded by the Science, Technology and Innovation Fund of the General Royalties System (SGR) of Colombia through the project called: "*Fortalecimiento de la cadena productiva de la zanahoria mediante la creación de prototipos de productos innovadores en el Oriente del departamento de Antioquia*" (code BPIN: 2020000100192) and Corporacion Colombiana de Investigacion Agropecuaria, Agrosavia.

Declarations

Competing interests

The authors declare no competing interests.

Declaration of competing interest

The authors declare that they have no known competing financial interests or personal relationships that could have appeared to influence the work reported in this paper.

Funding

This research was funded by the Science, Technology and Innovation Fund of the General Royalties System (SGR) of Colombia through the project called: "*Fortalecimiento de la cadena productiva de la zanahoria mediante la creación de prototipos de productos innovadores en el Oriente del departamento de Antioquia*" (code BPIN: 2020000100192) and the Colombian Agricultural Research Corporation—Agrosavia.

Additional information

Supplementary Information The online version contains supplementary material available at https://doi.org/10.1038/s41598-026-36993-2.

Correspondence and requests for materials should be addressed to J.M.-S. or J.C.H.-R.